Available online at www.sciencedirect.com
SCIENCE DIRECT®
Journal of Crystal Growth 260 (2004) 159–165
JOURNAL OF CRYSTAL GROWTH
www.elsevier.com/locate/jcrysgro

Crystal growth and properties of $(Lu,Y)_3Al_5O_{12}$

Yasuhiko Kuwano[a], Katsumi Suda[b], Nobuo Ishizawa[b,*], Toyoaki Yamada[c]

[a] *Functional Materials Research Laboratories, TNEC Corporation 4-1-1 Miyazaki, Miyamae-ku, Kawasaki 216-8555 Japan*
[b] *Materials and Structures Laboratory, Tokyo Institute of Technology, 4259 Nagatsuta, Midori-ku, Yokohama 226-8503, Japan*
[c] *National Industrial Research Institute of Nagoya, 1-1, Hitate-cho, Kita-ku, Nagoya 462-8510 Japan*

Received 27 June 2001; accepted 14 August 2003
Communicated by K. Nakajima

Abstract

LuYAG [$(Lu,Y)_3Al_5O_{12}$] single crystals have been grown by means of the Czochralski method. The solidification points of LuYAG ranged from 2010°C for $Lu_3Al_5O_{12}$ to 1930°C for $Y_3Al_5O_{12}$. Lattice parameters of LuYAG changed linearly with variations in composition from 11.9164(4) Å for $Y_3Al_5O_{12}$ to 12.0075(3) Å for $Y_3Al_5O_{12}$. The effective segregation coefficients k_{eff}, experimentally determined from the lattice parameters, show that compositional segregation of Y atoms proceeds with increasing Lu content. The heat capacity, heat diffusivity, and thermal conductivity of $Y_3Al_5O_{12}$, $Lu_2YAl_5O_{12}$, $Lu_{1.5}Y_{1.5}Al_5O_{12}$, $LuY_2Al_5O_{12}$ and $Y_3Al_5O_{12}$ were also measured. The two latter properties exhibit minima near the equimolar solid solution composition. Refractive indices, determined by the minimum deviation method, vary smoothly between 0.40 and 1.97 μm wavelengths and permit derivation of the Sellmeier constants.

Keywords: A1. Compositional segregation; A1. Heat capacity; A1. Heat diffusivity; A1. Refractive index; A1. Sellmeier constant; A1. Solid solutions; A1. Solidification points; A1. Thermal conductivity; B1. $Lu_3Al_5O_{12}$; B1. LuAG; B1. LuYAG; B1. Rare earth garnet; B1. $Y_3Al_5O_{12}$

1. Introduction

The solid solution $(Lu_xY_{1-x})_3Al_5O_{12}$ (LuYAG) series with the garnet-type structure have attracted much attention in laser applications. The end member compound LuAG (lutetium aluminum garnet, $Lu_3Al_5O_{12}$) is considered promising for quasi-three-level laser hosts. For example, Yb:LuAG (Yb-doped LuAG), is thought capable of providing a high efficiency diode-pumped laser [1–3]. The properties of the other end member compound YAG (yttrium aluminum garnet, $Y_3Al_5O_{12}$) are already well known. One reservation concerning the former end member is that the high purity Lu_2O_3 powders are very expensive from an industrial point of view. Another is that the solidification point of LuAG is extremely high for growth methods using crucibles. These difficulties vitiate the potential of LuAG crystals, and thus LuYAG crystals with reduced Lu concentration emerge naturally as alternatives [4].

There is another attractive feature of LuYAG crystals compared with LuAG when considered for laser-radar hosts in the 2 μm region [5,6]. The

*Corresponding author. Tel.: +81-45-924-5312; fax: +81-45-924-5360.
E-mail address: nishizaw@n.cc.titech.ac.jp (N. Ishizawa).

0022-0248/$ - see front matter © 2003 Elsevier B.V. All rights reserved.
doi:10.1016/j.jcrysgro.2003.08.060

centre lasing wavelength of 2022.7 nm for Tm:LuYAG with $x = 0.5$, i.e., $Lu_{1.5}Y_{1.5}Al_5O_{12}$, is longer than either 2020.3 nm of Tm:LuAG or 2013.3 nm of Tm:YAG [5]. This small difference in wavelength causes a significant reduction in the atmospheric absorption by H_2O and CO_2 gas, resulting in the transmission performance of Tm:LuYAG laser lights being superior to that of Tm:LuAG and much more for Tm:YAG [5,6].

Despite the many advantages of LuYAG in optical applications, their properties such as solidification points, segregation properties, thermal properties, and optical properties of the LuYAG solid solution crystals are not well established. In the present study, we first used a solar furnace to determine solidification points of LuYAG, and then grew LuYAG crystals by the Czochralski method and measured their lattice parameters, thermal and optical properties.

2. Experimental procedure

The solidification points of LuYAG solid solution were measured by digital pyrometry using a specular reflection method employing a heliostat solar furnace composed of parabolic mirror of 1.5 m in diameter and auxiliary flat square mirror of 2.4 m each side [7–9]. The five starting compositions; $Lu_3Al_5O_{12}$ ($x = 1$, LuAG), $Lu_2YAl_5O_{12}$ ($x = \frac{2}{3}$), $Lu_{1.5}Y_{1.5}Al_5O_{12}$ ($x = \frac{1}{2}$), $LuY_2Al_5O_{12}$ ($x = \frac{1}{3}$) and $Y_3Al_5O_{12}$ ($x = 0$, YAG), were prepared from a mixture of Lu_2O_3, Y_2O_3 and Al_2O_3 powders pressed at 98 MPa into $6 \times 6 \times 30\,mm^3$ square pillars.

First the upper part of the pillar was melted by centring the focal point of the solar furnace. The melt was then quenched by closing the solar light shutter. The change in radiative energy emitted from the melt was measured dynamically using the pyrometer (Minolta IR1362) [9]. The output voltage from the photomultiplier was recorded by an oscilloscope and transferred to computer. An example of a cooling curve thus obtained dynamically is shown in Fig. 1. The plateau of the curve corresponds to the solidification point [9]. The solidification temperature T_m (K) is dependent on the light wavelength $\lambda = 0.65\,\mu m$ and

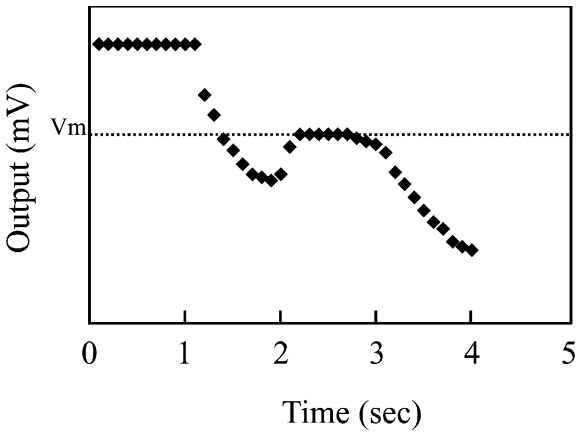

Fig. 1. Schematic cooling curve of a $(Lu_xY_{1-x})_3Al_5O_{12}$ melt.

calibration voltage $V_s = 0.3094$ V at the reference temperature $T_s = 2172$ K via the relation;

$$T_m = \frac{C_2}{\lambda \ln[\varepsilon(V_s/V_m)\{\exp(C_2/\lambda T_s) - 1\} - 1]}, \quad (1)$$

where V_m is the output voltage at the solidification point, ε the emissivity of the sample which will be discussed in Section 3.1, and the constant C_2 ($= 0.014388$ mK) originates from Plank's radiation law. The accuracy of T_m has been estimated to be approximately ± 2 K near 2200 K [7,9].

LuYAG single crystals were grown in a standard Czochralski (CZ) RF-heating apparatus, using an iridium crucible 50 mm in diameter, 50 mm in height and 2 mm in thickness. Raw materials were Lu_2O_3, Y_2O_3 and Al_2O_3 powders of 99.999% purity. The charged weight was 450 g. Initial compositions were identical to those prepared for the solidification point measurements. Growth was seeded along the crystallographic [1 1 1] direction and conducted under N_2 with 150 ppm O_2 mixture gas flow atmosphere.

Lattice parameters of the grown crystals were determined with a four-circle rotating anode X-ray diffractometer (Rigaku AFC5R), employing Ag Kα radiations and a LiF (0 0 2) monochromater. Specimens were cut from the rod and ground into spheres of approximately 0.1 mm in diameter. Twenty-five reflections within the 2θ range of 48–58° were used for the determination of the lattice parameter a for each sample. For the mixed

crystals with nominal composition of $LuY_2Al_5O_{12}$, $Lu_{1.5}Y_{1.5}Al_5O_{12}$ and $Lu_2YAl_5O_{12}$, specimens were collected from the slices cut perpendicular to the growth direction to determine the effective segregation coefficients k_{eff}. The position of a slice with respect to the whole crystal rod was characterised by the solidified fraction g [10].

The heat capacity (c) and heat diffusivity (κ) of LuYAG were measured by the laser-flash method using a Shinku Rikou (ULVAC) TC7000. The samples were shaped into rods 10 mm in diameter and 5 mm in length. The top and bottom surfaces were polished with #1200 alumina powder and etched with hot phosphoric acid at 250°C, for 1 h. The crystal densities (ρ) were measured by the Archimedes method. The thermal conductivity (k) was calculated from $k = \kappa c \rho$. The uncertainty for the thermal conductivity was estimated to be ± 0.2 W/mK.

The minimum deviation method [11,12] was used to measure the crystal refractive indices. Since the LuYAG crystals all have a cubic structure and are optically isotropic, only one prism was needed for each measurement. Five prisms of different compositions were prepared from the grown crystals. They were cut from the crystal rod at $g = 0.15-0.20$. The vertical angle α of each prism was 40° and the light accepting face was $10 \times 10\,mm^2$. The refractive indices (n) were calculated from the relation:

$$n = \frac{\sin((\alpha + \delta)/2)}{\sin(\alpha/2)}, \quad (2)$$

where δ is the measured minimum deviation angle. Measurements were made at a room temperature of 24.7 ± 1°C and pressure of 103.25 hPa.

3. Results and discussion

3.1. Solidification points

It is always a matter of argument whether the emissivity ε has been evaluated correctly in determining solidification points via pyrometry. Yamada [9] reported $\varepsilon = 0.96$ for YAG, but because the emissivity of LuAG could not be identified from the literature, we have assumed the value $\varepsilon = 0.87$ reported for $Yb_3Al_5O_{12}$ garnet [7,9], bearing similarities in terms of both ionic radii and atomic numbers of the Lu and Yb constituents. We further assumed the linear variation of ε from 0.96 to 0.87 across the entire range of LuYAG solid solutions studied.

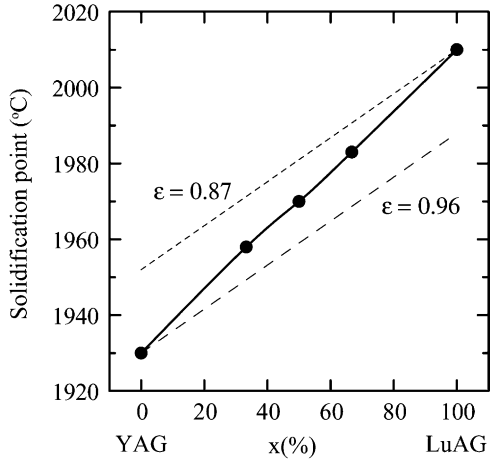

Fig. 2. Estimated solidification point T_m (solid line) of the $(Lu_xY_{1-x})_3Al_5O_{12}$ solid solution. The dashed lines indicate those assuming $\varepsilon = 0.87$ for LuAG and $\varepsilon = 0.96$ for YAG over the entire compositions.

The solidification temperatures thus obtained were: 2010°C for $Lu_3Al_5O_{12}$, 1983°C for $Lu_2YAl_5O_{12}$, 1970°C for $Lu_{1.5}Y_{1.5}Al_5O_{12}$, 1958°C for $LuY_2Al_5O_{12}$, and 1930°C for $Y_3Al_5O_{12}$. The variation of T_m as a function of Lu content x in $(Lu_xY_{1-x})_3Al_5O_{12}$ is plotted in Fig. 2. Two parallel dashed lines indicate ideal limiting solidification temperatures assuming $\varepsilon = 0.87$ and 0.96 for all the compounds in the system. The solidification temperature increases almost linearly with increasing Lu content.

3.2. Crystal growth

All the grown crystals were colourless and of laser grade crystal quality. Fig. 3 shows an example of a grown LuYAG crystal. Stable growth was attained with the pulling rate of 2 mm/h and the rotation rate of 14 rpm. The sizes of the grown crystals were 15–25 mm in diameter and 40–80 mm in length. As noted

in Section 3.1, the solidification point of LuYAG increases with increasing Lu content in the melt. To cope with the increasing temperatures, the thickness of zirconia heat shielding atop the crucible was increased from 4 mm for YAG to 10 mm for LuYAG.

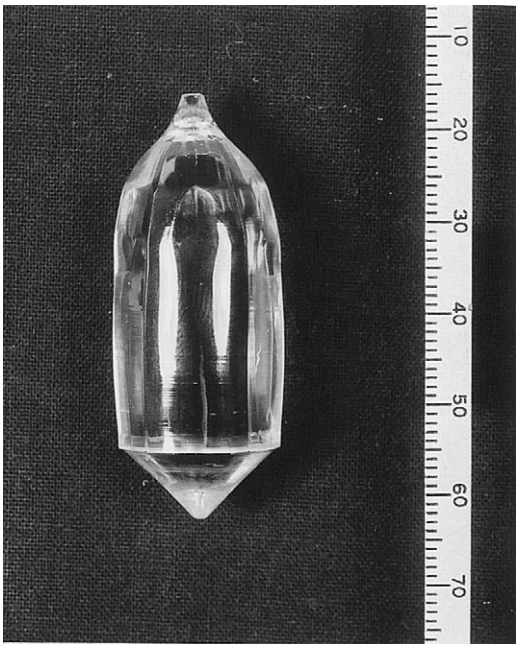

Fig. 3. Photograph of $Lu_{1.5}Y_{1.5}Al_5O_{12}$ single crystal.

3.3. Lattice parameters

The crystal lattice parameters are given in Table 1. They decrease almost linearly with increasing Lu content x in $(Lu_xY_{1-x})_3Al_5O_{12}$. Assuming the Vegard's law [13], the true composition was calculated from the lattice parameter a in Å using an approximation, $a = 12.0075 - 0.0911x$. The calculated compositions of the mixed crystals deviate from the melt composition by at most 5% in x, as indicated in Table 1. Variation of the lattice parameters of LuYAG solid solution as a function of x is plotted in Fig. 4.

To determine the compositional segregation in LuYAG, the effective segregation coefficients for Y atoms were estimated using the equation;

$$k_{\text{eff}} = \frac{\log(C_1/C_2)}{\log((1-g_1)/(1-g_2))} + 1, \tag{3}$$

where the values of C_n ($n = 1$ and 2) are the Y_2O_3 concentrations at the solidified fractions g_n [10]. The k_{eff} values are also given in Table 1. As shown in Fig. 5, k_{eff} for Y decreases quadratically with increasing Lu_2O_3 content.

3.4. Thermal properties of LuYAG

Thermal properties including heat capacity, heat diffusivity, and thermal conductivity, as well as the results of density measurements are summarised in Table 2. The heat capacity decreased

Table 1
Lattice parameters, composition, and segregation coefficients of $(Lu_xY_{1-x})_3Al_5O_{12}$ crystals

Crystals	Initial composition x (%)	g	Lattice parameter a (Å)	Calculated composition x (%)	k_{eff} (for Y)
$Y_3Al_5O_{12}$	0	—	12.0075(3)	—	—
$LuY_2Al_5O_{12}$	33.3	0.001 0.525	11.9765(4) 11.9796(2)	34.2 30.9	0.94
$Lu_{1.5}Y_{1.5}Al_5O_{12}$	50.0	0.007 0.467	11.9575(3) 11.9611(3)	54.9 51.1	0.89
$Lu_2YAl_5O_{12}$	66.7	0.002 0.141	11.9431(3) 11.9438(4)	70.8 69.9	0.79
$Lu_3Al_5O_{12}$	100.0	—	11.9164(4)	—	—

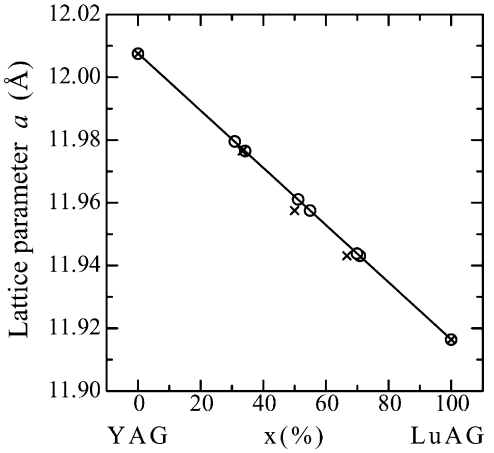

Fig. 4. Lattice parameter of $(Lu_xY_{1-x})_3Al_5O_{12}$ solid solution. The open circles are those with calibrated compositions based on the Vegard's law, and the crosses are those without corrections.

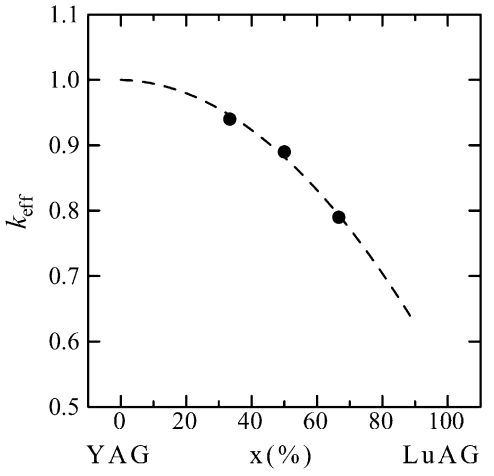

Fig. 5. Effective segregation coefficients k_{eff} for Y atoms of $(Lu_xY_{1-x})_3Al_5O_{12}$ crystals, with a dashed curve fitted by a quadric function passing through the point $k_{eff} = 1$ at YAG composition for viewing convenience.

monotonically with increasing Lu_2O_3 content while both the thermal conductivity and heat diffusivity have a concave in the middle of the solid solution, latter of which is shown in Fig. 6.

The significant reduction of thermal conductivity near the equimolar fraction in garnet-type mixed crystals are also reported for GGAG

Table 2
Heat capacity, heat diffusivity, thermal conductivity and density of $(Lu_xY_{1-x})_3Al_5O_{12}$ crystals

Crystals	Heat capacity (J/gK)	Heat diffusivity (cm^2/s)	Density (g/cm^2)	Thermal conductivity (W/mK)
$Y_3Al_5O_{12}$	0.603	0.0473	4.53	12.9
$LuY_2Al_5O_{12}$	0.572	0.0275	5.37	7.8
$Lu_{1.5}Y_{1.5}Al_5O_{12}$	0.481	0.0275	5.64	7.5
$Lu_2YAl_5O_{12}$	0.475	0.0275	6.01	7.6
$Lu_3Al_5O_{12}$	0.411	0.0347	6.72	9.6

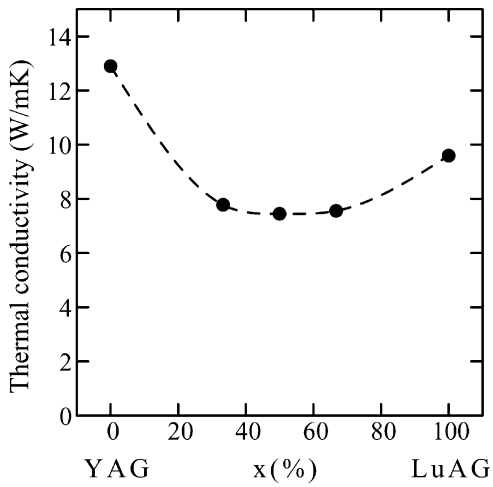

Fig. 6. Thermal conductivity (k) of $(Lu_xY_{1-x})_3Al_5O_{12}$ solid solution, with dashed line fitted to the observed k values by a spline function for viewing convenience.

($Gd_3Ga_5O_{12}$–$Gd_3Al_5O_{12}$ solid solution system) [12], and YIAG ($Y_3Fe_5O_{12}$–$Y_3Al_5O_{12}$ solid solution system) [14]. These phenomena reflect the enhanced scattering of phonons due to microscopic strains introduced in the mixed crystal lattice, which originates in the difference in chemical bond strength of the host and substitutional solute atoms.

3.5. Refractive indices of LuYAG

The results of refractive index measurements for LuYAG are summarised in Table 3 and plotted in Fig. 7 as a function of wavelength. The accuracy of

Table 3
Refractive indices of $(Lu_xY_{1-x})_3Al_5O_{12}$ crystals

λ (nm)	$Y_3Al_5O_{12}$	$LuY_2Al_5O_{12}$	$Lu_{1.5}Y_{1.5}Al_5O_{12}$	$Lu_2YAl_5O_{12}$	$Lu_3Al_5O_{12}$
1970.09	1.80092	1.80433	1.80608	1.80805	1.81079
1529.58	1.80730	1.81066	1.81239	1.81432	1.81703
1013.98	1.81566	1.81896	1.82067	1.82256	1.82523
852.11	1.81968	1.82296	1.82466	1.82654	1.82919
706.52	1.82519	1.82844	1.83012	1.83198	1.83461
587.56	1.83264	1.83586	1.83752	1.83935	1.84194
486.13	1.84371	1.84687	1.84850	1.85030	1.85284
404.66	1.85975	1.86283	1.86441	1.86616	1.86862

measured values is $\pm 1 \times 10^{-5}$. The smooth curves in Fig. 7 are strong indicators of compositional homogeneity and good crystalline quality. The refractive indices become large with increasing Lu content at a constant wavelength in the range studied. Changes of the refractive index against wavelength followed the Sellmeiyer relation [15]:

$$n^2 - 1 = \frac{A_1\lambda^2}{\lambda^2 - B_1} + \frac{A_2\lambda^2}{\lambda^2 - B_2} + \frac{A_3\lambda^2}{\lambda^2 - B_3}, \quad (4)$$

where the Sellmeier constants A_n and B_n were determined by fitting and listed in Table 4.

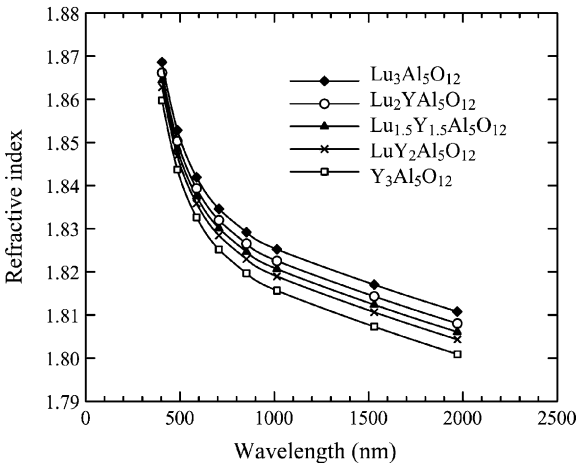

Fig. 7. Changes of refractive indices of $(Lu_xY_{1-x})_3Al_5O_{12}$ crystals as a function of wavelength.

4. Summary

Optical grade single crystals of $Lu_3Al_5O_{12}$ (LuAG), $Lu_2YAl_5O_{12}$ (Lu:Y = 2:1), $Lu_{1.5}Y_{1.5}Al_5O_{12}$ (Lu:Y = 1:1), $LuY_2Al_5O_{12}$ (Lu:Y = 1:2) and $Y_3Al_5O_{12}$ (YAG) in the LuYAG solid solution series were grown by the CZ method, and their optical and themal properties were measured. The main results are as follows:

(1) The solidification points of LuYAG crystals were measured by the digital pyrometry using a solar furnace. They changed almost linearly from 1930°C (YAG) to 2010°C (LuAG) in the solid solution range.
(2) Lattice parameters of LuYAG vary almost linearly with changes in composition from 11.9164(4) Å (LuAG) to 12.0075(3) Å (YAG). The effective segregation coefficient k_{eff} were estimated for the LuYAG crystals. They changed quadratically with increasing Lu content.
(3) The heat capacity decreased monotonically with increasing Lu content from 0.603 (YAG) to 0.411(LuAG) J/gK. The thermal conductivity and heat diffusivity exhibit minima near the equimolar composition due to the enhanced scattering of phonons by the microstrains caused by substitution.
(4) Refractive indices were measured in the wavelength range between 0.41 and 1.97 μm from which the Sellmeier constants were obtained. The refractive indices increase smoothly from 1.80 to 1.87 with decreasing wavelength.

Table 4
Sellmeier coefficients for $(Lu_xY_{1-x})_3Al_5O_{12}$ crystals ($0.41 < \lambda < 1.97\,\mu m$)

Coeff.	$Y_3Al_5O_{12}$	$LuY_2Al_5O_{12}$	$Lu_{1.5}Y_{1.5}Al_5O_{12}$	$Lu_2YAl_5O_{12}$	$Lu_3Al_5O_{12}$
A1	1.28040E+00	1.20249E+00	1.77362E+00	1.62592E+00	1.47199E+00
A2	1.00244E+00	1.09230E+00	5.27323E−01	6.81944E−01	8.45642E−01
A3	4.57401E+00	4.23947E+00	3.87734E+00	4.25673E+00	3.82124E+00
B1	5.49568E−03	1.79270E−02	7.90836E−03	7.07742E−03	6.21359E−03
B2	1.92189E−02	4.29592E−03	2.31844E−02	2.15148E−02	2.00432E−02
B3	3.87058E+02	3.61709E+02	3.32469E+02	3.66181E+02	3.30483E+02

References

[1] T. Kasamatsu, H. Sekita, Y. Kuwano, Appl. Opt. 38 (1999) 5149–5153.
[2] D.S. Sumida, Tech.Digest, Adv. Solid State Lasers (1995) 224–226.
[3] D.W. Hart, Opt. Lett. 21 (1996) 728.
[4] A.I. Zagumennyi, Yu.D. Zarartsev, P. Asudenikin, V.I. Vlasov, V.A. Kozlov, A.F. Umyskov, Optical Soc. Amer. Tops. Adv. Solid State Lasers (1996) 100–101.
[5] J.D. Kmetec, T.S. Kubo, T.J. Kane, Opt. Lett. 19 (1994) 186–188.
[6] L.S. Rothman, R.R. Gamache, A. Goldman, L.R. Brown, R.A. Toth, H.M. Picket, R.L. Poynter, J.M. Flaud, C. Camy-Peyret, A. Barbe, N. Husson, C.P. Rinsland, M.A.H. Smith, Appl. Opt. 26 (1987) 4058.
[7] M. Mizuno, T. Yamada, Report of Government Industrial Research Institute, Vol. 34(7), Nagoya, 1985, pp. 222–228.
[8] M. Mizuno, T. Yamada, T. Noguchi, Yogyou-kyoukai-Shi 90 (1982) 335–337 (in Japanese).
[9] T. Yamada, Construction of temperature measurement system for light furnaces and its application to refractory ceramic materials, Ph.D. Thesis, Tokyo Institute of Technology, 1998, pp. 26–49 (in Japanese).
[10] B.R. Pamplin, Crystal growth, Pergamon Press, New York, 1975, pp. 2–9.
[11] Y. Kuwano, J. Appl. Phys. 49 (1978) 4223–4224.
[12] Y. Kuwano, S. Saito, U. Hase, J. Cryst. Growth 92 (1988) 17–22.
[13] L. Vegard, Z. Phys. 5 (1921) 17–26.
[14] N.P. Padture, P.G. Klemens, J. Amer. Ceram. Soc. 80(4) (1997) 1018–1020.
[15] M. Born, E. Wolf, Principles of Optic, Pergamon Press, New York, 1980, pp. 96–97.